ANNUAL REPORT 2012

UIUC, August 16, 2012

Multiphase Model of Precipitate Formation and Grain Growth in Continuous Casting

Kun Xu
(Ph.D. Student)

Department of Mechanical Science and Engineering
University of Illinois at Urbana-Champaign

Temperature zones of low hot ductility of steel related to precipitate embrittlement

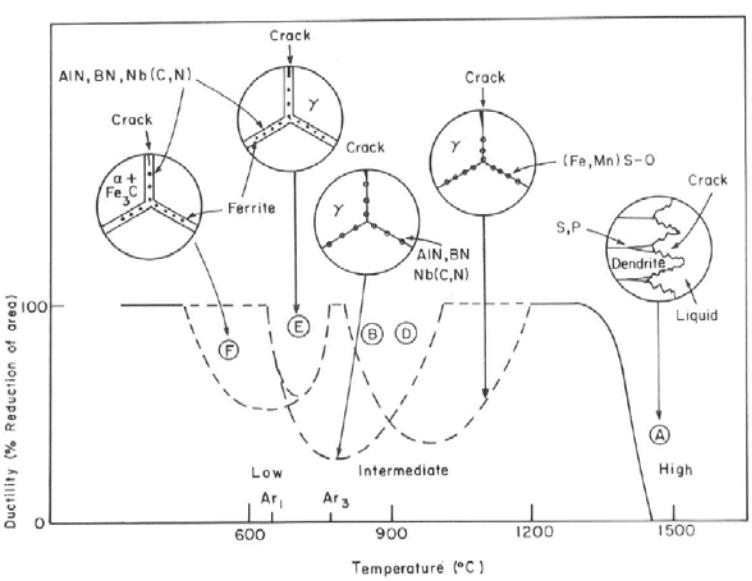

B.G. Thomas *et al*, *ISS Transactions*, 1986, pp. 7.

- Precipitate embrittlement is an important reason for reduced hot ductility
- The different temperature zones for ductility troughs are related to stability of different precipitates in steel
- Low ductility during $\gamma \rightarrow \alpha$ phase transformation is caused by an accelerating precipitation (interphase fine precipitates), or weak ferrite films on austenite grain boundaries

Factors affecting hot ductility

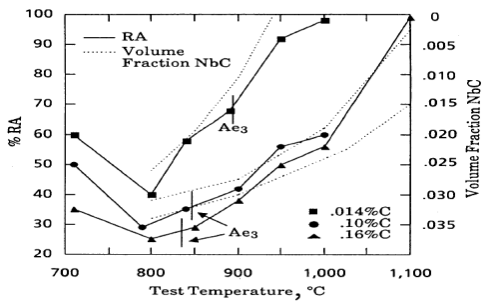

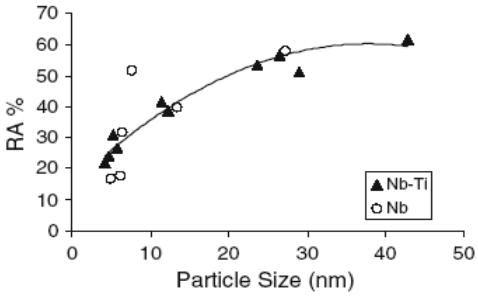

B.Mintz *et al*, *Inter. Mater. Rev.*, 1991, pp. 187.

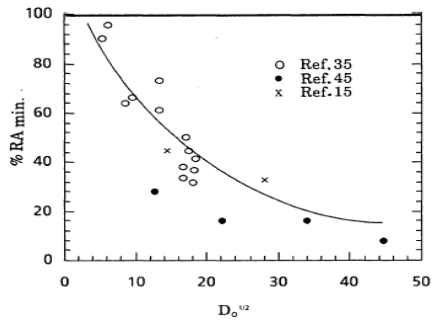

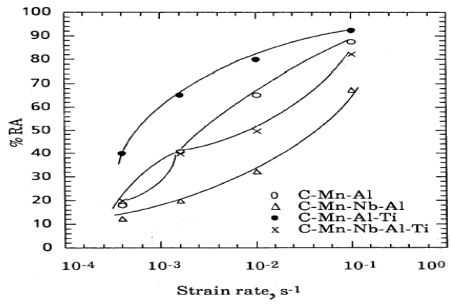

K. R. Carpenter *et al*, *Metall. Mater. Trans. A*, 2009, p. 503.

➢ Hot ductility in intermediate-temperature zone decreases with larger precipitate amount, finer precipitate size, coarser grain size and smaller strain rate

Project overview

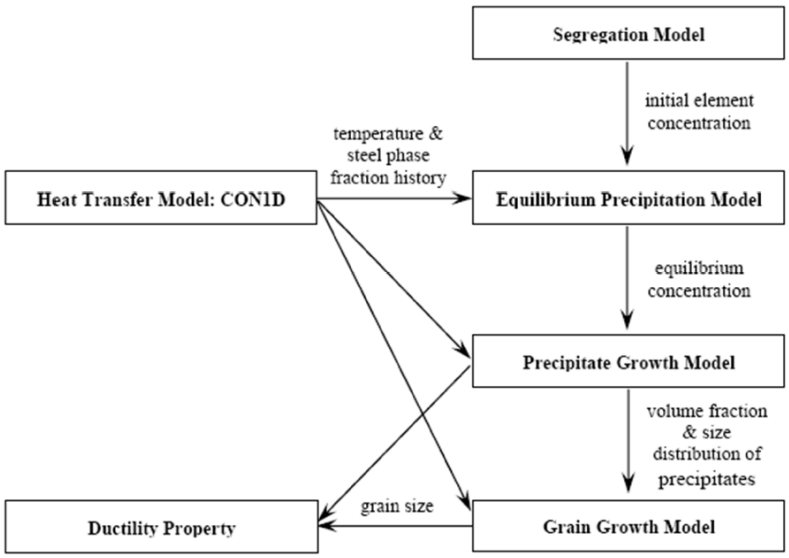

Final goal: Design casting practices to prevent transverse cracks

Equilibrium precipitation model

To solve a system of nonlinear equations, which includes:

1. Solubility limits for 18 precipitates with activities from Wagner interaction between elements
2. Mass balance for 13 alloying elements during precipitation
3. Mutual solubility, e.g. (Ti,Nb,V)(C,N)

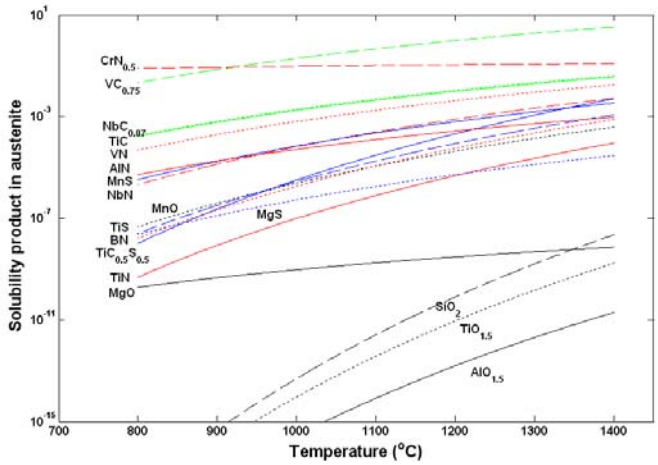

Calculate amount of stable precipitate phases and dissolved concentrations of elements at equilibrium in microalloyed steels for the given temperature and steel grade

K. Xu, B. G. Thomas and Ron O'Malley, *Metall. Mater. Trans.* A, 2011, vol. 42A, pp. 524

Classical definition of precipitation

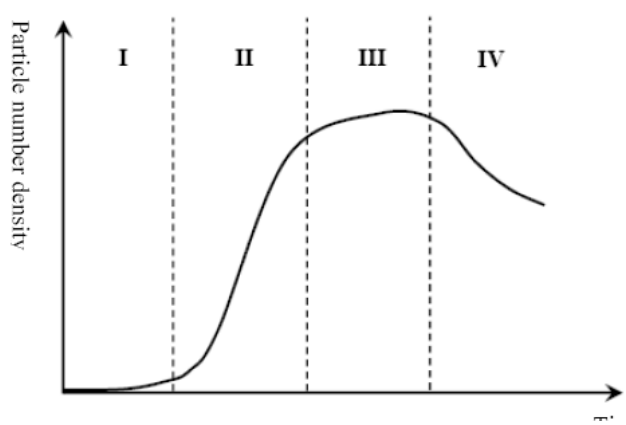

I. Induction: waiting time for stable nuclei to form

II. Nucleation: stable nuclei are continuously generated

III. Growth: all particles can grow driven by high supersaturation

IV. Coarsening: large particles grow while small particles shrink when supersaturation is at equilibrium

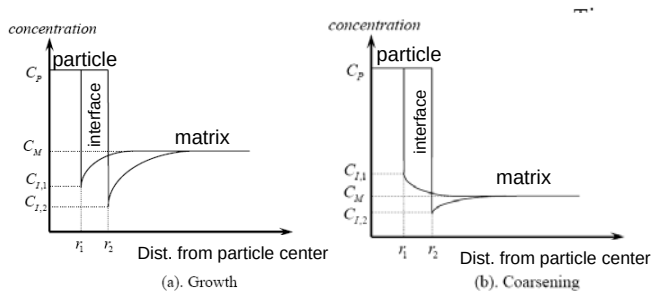

- Interface concentration decreases with increasing particle size, and matrix concentration decreases to be between interface concentrations of large and small particles

Models of precipitation kinetics

- Single-phase precipitation:

1. Classical precipitation model (Becker and Döring: Nucleation, Zener: Growth, LSW: Coarsening, MLS model, KWN model)

2. Kinetic Monte Carlo model 3. Phase Field method 4. Cluster Dynamics

- Multiphase precipitation:

1. PRISMA (KWN model) --- Thermo-Calc Software and QuesTek LLC
2. Multiphase Field method
3. Matcalc (thermodynamic extremum principle)

Our new developing model:

1. It simulates nucleation, growth/dissolution and coarsening as one continuous and competing process, and no explicit laws and fitting parameters are required
2. The particles of every size are tracked, ranging from single pseudomolecule, unstable embryos, stable nuclei to very large coarsened particles

Multiphase precipitation model

For each size particle : average molar fraction of each precipitate phase (p_i^z, z=1,2,…, n_p) and number density (n_i) of variable-composition particles

- Mutually-exclusive precipitates

$$\frac{d(p_i^z n_i)}{dt} = -\beta_i^z n_1^z p_i^z n_i - \alpha_i^z A_i p_i^z n_i + \beta_{i-1}^z n_1^z p_{i-1}^z n_{i-1} + \alpha_{i+1}^z A_{i+1} p_{i+1}^z n_{i+1} \ (i \geq 2) \ (z=1,2,\ldots,n_p)$$

$$\frac{d(n_1^z)}{dt} = -n_1^z \sum_{i=1}^{i_M} (1+\delta_{1,i}) \beta_i^z p_i^z n_i + \sum_{i=2}^{i_M} (1+\delta_{2,i}) \alpha_i^z A_i p_i^z n_i \quad (z=1,2,\ldots,n_p)$$

- Mutually-soluble precipitates

$$\frac{d(p_i^z n_i)}{dt} = -\sum_{s=1}^{n_P} \beta_i^s n_1^s p_i^z n_i + \sum_{s=1}^{n_P} \beta_{i-1}^s n_1^s n_{i-1} \frac{(i-1) p_{i-1}^z + \delta_{s,z}}{i} - \sum_{s=1}^{n_P} \alpha_i^s A_i p_i^z n_i$$

$$+ \sum_{s=1}^{n_P} \alpha_{i+1}^s A_{i+1} n_{i+1} \frac{(i+1) p_{i+1}^z - \delta_{s,z}}{i} \quad (i \geq 2) \ (z=1,2,\ldots,n_p)$$

$$\frac{dn_1^z}{dt} = -\beta_1^z n_1^z \sum_{s=1}^{n_p} n_1^s - n_1^z \sum_{s=1}^{n_p} \beta_1^s n_1^s - \beta_i^z n_1^z \sum_{i=2}^{i_M} n_i + 2 \sum_{s=1}^{n_p} a_2^s A_2 p_2^z n_2 + \sum_{i=3}^{i_M} \alpha_i^z A_i n_i$$

For mutually-soluble precipitates, pseudomolecules from all precipitate phases have influence on both diffusion growth and dissolution.

Test Problem: Mutually-exclusive precipitates (e.g. AlN and NbC)

Dimensionless form $n_i^* = n_i / n_{1,eq}$ $t^* = 4\pi D_1 r_1 n_{1,eq} t$

Pseudomolecules produced by an isothermal first order reaction

$$n_s^A(t^*) = \sum_{i=1}^{i_M} i \cdot p_i^A n_i = 9 n_{1,eq}^A [1 - \exp(-0.1 t^*)]$$

$$n_s^B(t^*) = \sum_{i=1}^{i_M} i \cdot p_i^B n_i = 9 n_{1,eq}^B [1 - \exp(-0.1 t^*)]$$

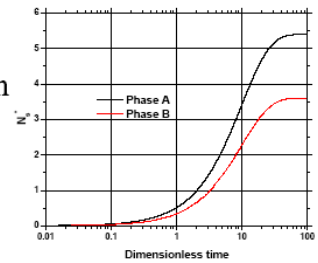

$n_{1,eq}^A = 3.6\times10^{23}\#/\mathrm{m}^3$, $n_{1,eq}^B = 2.4\times10^{23}\#/\mathrm{m}^3$, $n_{1,eq} = n_{1,eq}^A + n_{1,eq}^B = 6\times10^{23}\#/\mathrm{m}^3$

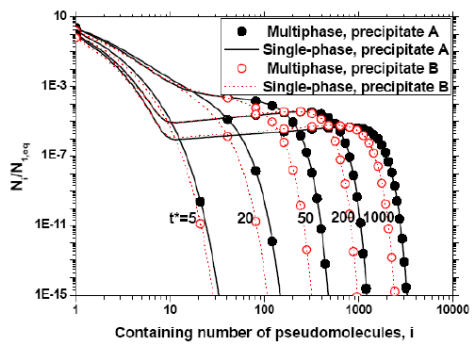

(a). Particle size distributions

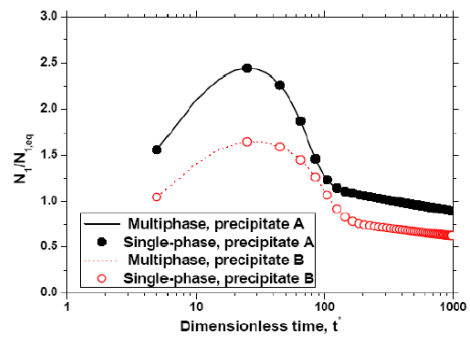

(b). Number densities of single pseudomolecules

Test Problem: Mutually-soluble precipitates (e.g. $Al^{27}N$ and $Al^{26}N$)

Choose the same parameters as those in mutually-exclusive precipitates test problem, a single-phase model is run by taking

$$n_s(t) = n_s^A(t) + n_s^B(t) \text{ and } n_{1,eq} = n_{1,eq}^A + n_{1,eq}^B$$

The results from single-phase model are multiplied by molar fractions 0.6 and 0.4 to get particles number densities of each precipitate phase, and compared with results of multiphase model

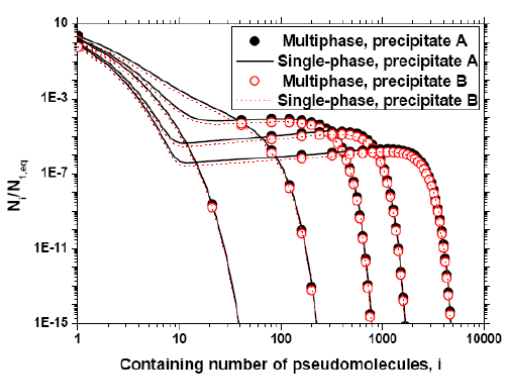

(a). Particle size distributions

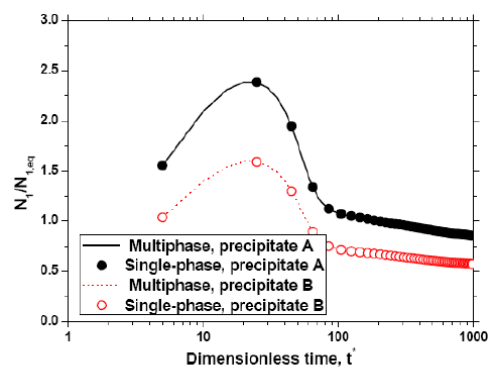

(b). Number densities of single pseudomolecules

Comparison of size distributions for mutually-exclusive and mutually-soluble precipitates

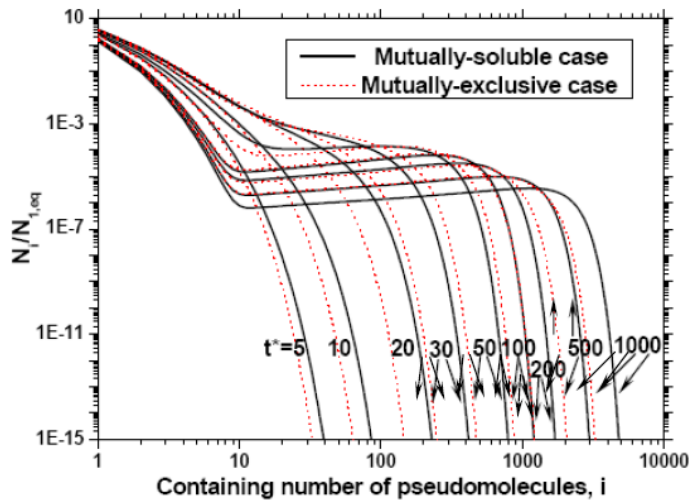

- All input values are the same for two test problems
- Mutually-soluble precipitates give larger size because the particles can be supported as the nucleation and growth sites to attract pseudomolecules of both precipitate phases

Introduction of Particle-Size-Grouping (PSG) Method

- The model always simulates from single pseudomolecule (~ 0.1nm) up to large coarsened particles (~100μm): particles could contain 1-10^{18} pseudomolecules
- Serious computation and memory storage issues arise with such a large size range
- Solve with PSG method: Use N_G groups (<100) of geometrically progressing size

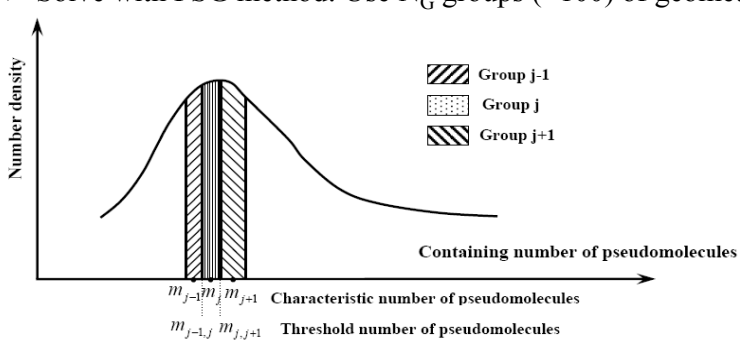

m_j: Characteristic number of pseudomolecules for size group j particle

$m_{j,j+1}$: Threshold number of pseudomolecules to separate size group j and j+1 particles

$$m_{j,j+1} = \sqrt{m_j m_{j+1}}$$

Total number density of each size group $N_j = \sum_{m_{j,j+1} > m > m_{j-1,j}} n(m)$

Average molar fraction of each phase $P_j^s = \dfrac{\sum_{m_{j,j+1} > m > m_{j-1,j}} m \cdot n(m) \cdot p_m^s}{\sum_{m_{j,j+1} > m > m_{j-1,j}} m \cdot n(m)}$

Average particle ratio

$$R_V = m_{j+1} / m_j$$

PSG method for mutually-soluble precipitates

$$\frac{d(P_j^z N_j)}{dt} = \underbrace{\frac{m_1}{m_j}\beta_j^z N_1^z (N_j - n_j^R)}_{\text{Diffusion growth inside group j}} - \underbrace{\frac{m_1}{m_j}\alpha_j^z A_j (N_j - n_j^L)}_{\text{Dissolution inside group j}}$$

$$+\underbrace{\sum_{s=1}^{n_p}(\beta_{j-1}^s)^R N_1^s n_{j-1}^R \frac{floor(m_{j-1,j})(P_{j-1}^z)^R + \delta_{s,z}}{m_j}}_{\text{Diffusion growth group j-1→j}} + \underbrace{\sum_{s=1}^{n_p}(\alpha_{j+1}^s)^L A_{j+1}^L n_{j+1}^L \frac{ceil(m_{j,j+1})(P_{j+1}^z)^L - \delta_{s,z}}{m_j}}_{\text{Dissolution group j+1→j}}$$

$$-\underbrace{\frac{floor(m_{j,j+1})}{m_j}\sum_{s=1}^{n_p}(\beta_j^s)^R N_1^s (P_j^z)^R n_j^R}_{\text{Diffusion growth group j→j+1}} - \underbrace{\frac{ceil(m_{j-1,j})}{m_j}\sum_{s=1}^{n_p}(\alpha_j^s)^L A_j^L (P_j^z)^L n_j^L}_{\text{Dissolution group j→j-1}} \quad (j \geq 2)\ (z=1,2,\ldots,n_p)$$

- Estimations of total number densities and molar fractions of different precipitate phases at border sizes (near threshold between neighboring size groups) are required

Application: Continuous Casting and Reheating

- The effects of microalloy precipitation and dissolution during direct strip production are explored relative to the position within the slab and alloy content
- Niobium solute in solution and precipitate form are quantified by electrochemical extraction and inductively coupled plasma, and the precipitate size are measured by transmission electron microscopy on carbon extraction replicas
- The extent of precipitation appears greatest with higher niobium additions. The greatest amount of alloy precipitation occurs at the slab surface, and the columnar region represents the bulk of the slab volume and exhibits the lowest precipitated amount

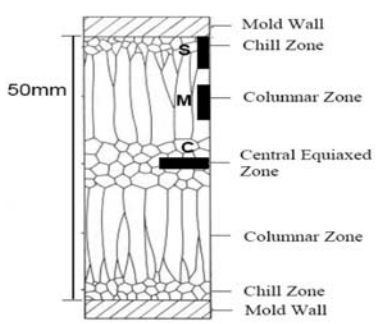

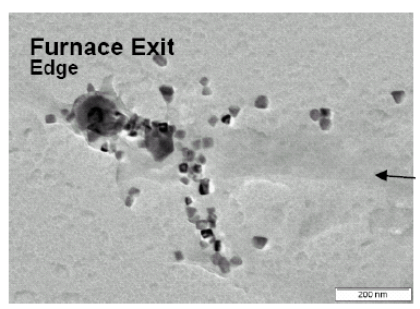

Experiment from: M. S. Dyer, *M. S. thesis*, Colorado School of Mines, 2010.

Steel Phase (CON1D)

CON1D program: Solve the transient heat conduction in the mold and spray regions of continuous steel slab casters using finite difference method

Steel	C	Mn	Si	Cr	Ti	Nb	V	Al	N	S	P
High-Nb	0.031	1.039	0.194	0.032	0.002	0.046	0.001	0.031	0.006	0.003	0.012

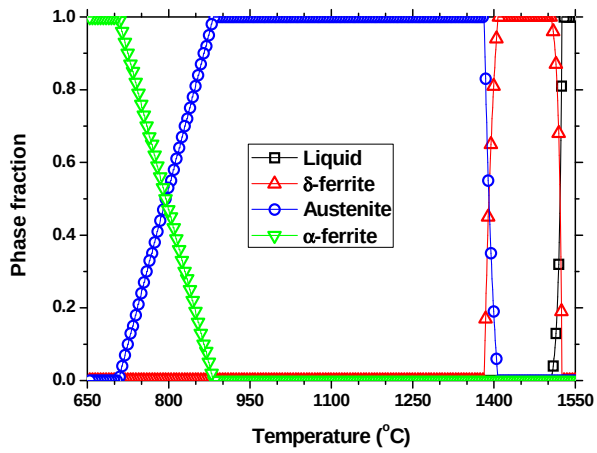

Slab size: 50mm thick, 1500mm wide
Mold exit: 0.8m below meniscus
Pouring Temperature: 1553°C
Casting speeds: 5m/min
Spray zone: 0.8-6 m below meniscus

Liquidus temperature: 1524.4°C
Solidus temperature: 1504.8°C
Highest temperature of totally austenite phase: 1381.8°C

Equilibrium Precipitation Calculation

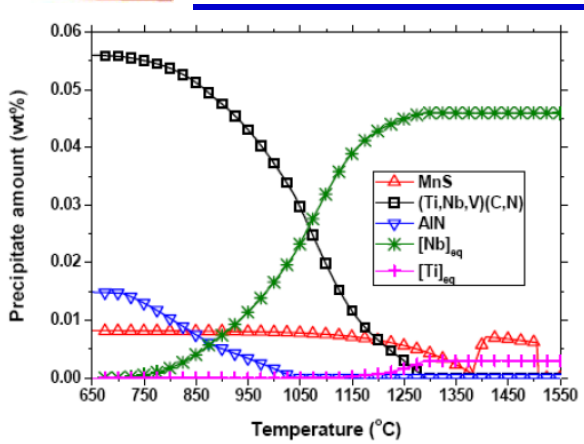

(a). Precipitate phases and amounts

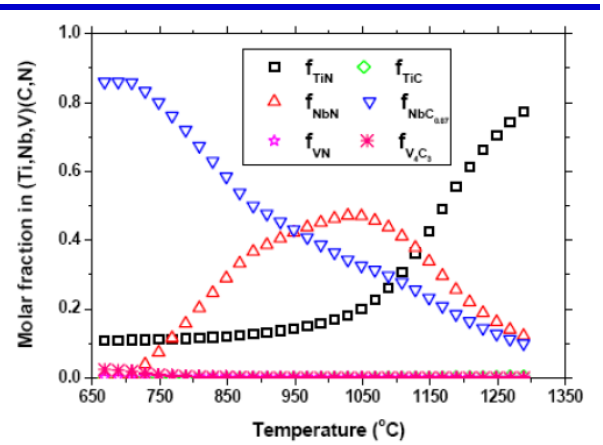

(b). Molar fractions in mixed (Ti,Nb,V)(C,N) precipitates

- Stable TiN is the main precipitate phase at high temperature, and more $NbC_{0.87}$ continues to precipitate out with lowering temperature
- Molar fractions of VN and V_4C_3 are always small, mixed (Ti,Nb,V)(C,N) precipitates are modeled as two mutually-soluble phases, Ti(C,N) and Nb(C,N)

Temperature history (casting+reheating)

- **Casting→Transfer→Reheating→Quenching**
- **After the end of spray cooling, slab is air cooled for 4m, then heated in a 225-m long reheating furnace with reference temperature 1150°C, and finally water quenched to room temperature 25°C**

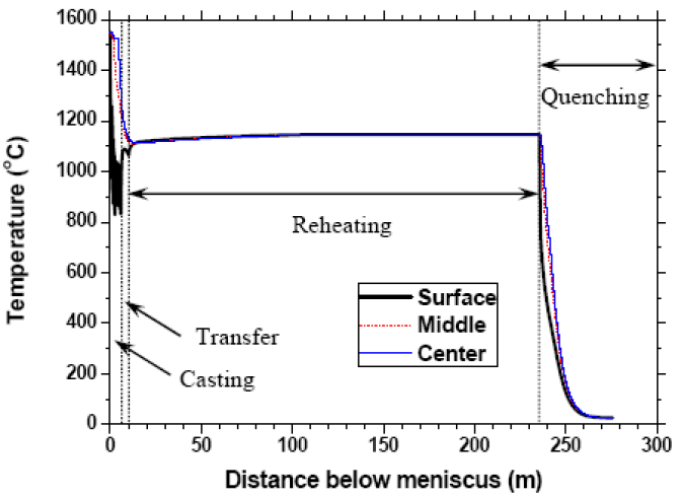

convection heat transfer coefficient of air $h=8.7W/(m^2K)$

heat transfer coefficient of agitated water $h=2000W/(m^2K)$

Single-phase model: particle size distributions of Nb(C,N)

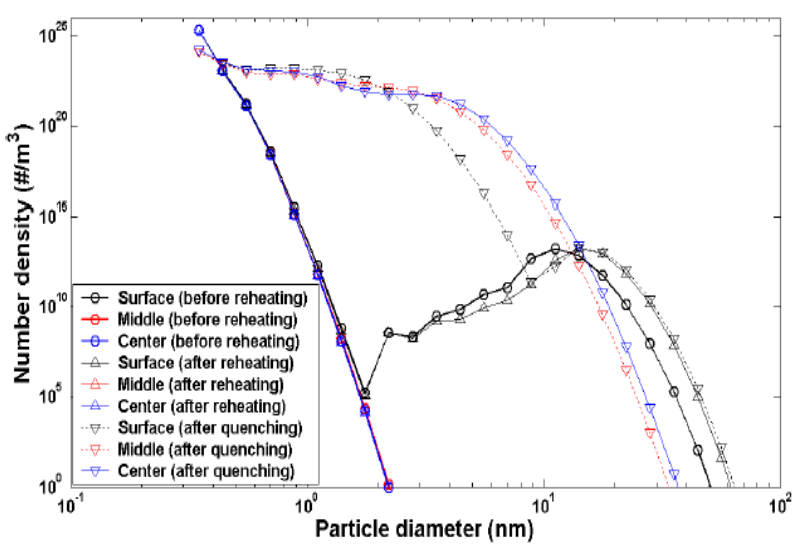

- For slab surface, Nb(C,N) begins to precipitate before reheating, and continue to grow in the reheating furnace (coarsening)
- For slab interior, Nb(C,N) can not get enough supersaturation to precipitate out before quenching. It begins to precipitate in quenching, mainly due to γ→α phase transformation

$D_{Nb}(m^2/s)=0.83\times10^{-4}\exp(-266500/RT)$ (in austenite), $D_{Nb}(m^2/s)=50.2\times10^{-4}\exp(-252000/RT)$ (in ferrite)
$D=f_\gamma D_\gamma+f_\alpha D_\alpha$, $\sigma_{Nb(C,N)}=0.5J/m^2$

Single-phase model: Comparison of size distributions

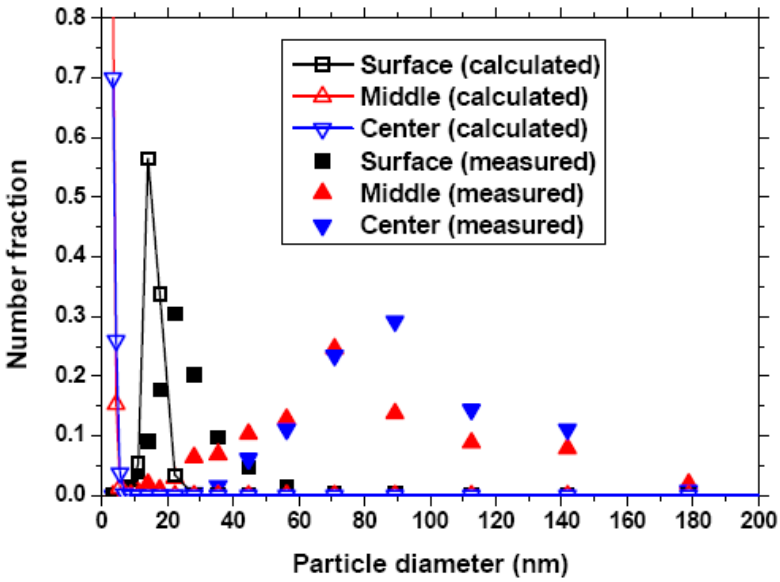

Compare average precipitate size

- Surface: calculated 14nm vs measured 24nm
- Middle: calculated ~3nm vs measured 72nm
- Center: calculated ~3nm vs measured 91nm

- Need explanations for much larger measured precipitate size for slab interior: existence of stable TiN and its mutually solubility with Nb(C,N)

Particle size distribution (casting+reheating)

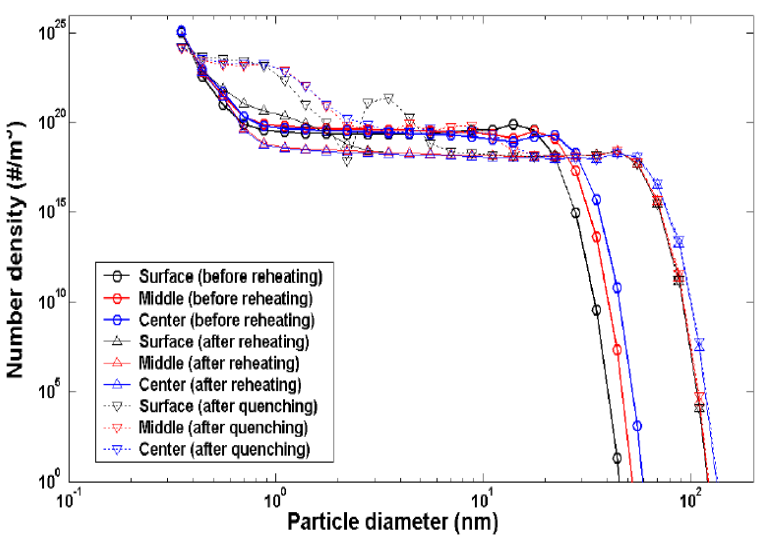

- Two-phase model for Ti(C,N) and Nb(C,N)
- A much larger precipitate size is predicted
- Reason: TiN is much more stable, and form at higher temperature to form large Ti-bearing particles. Nb(C,N) can precipitate on the surface of TiN due to their mutually solubility to make particles even larger
- 0.003wt% Ti addition is important (vs 0.046%Nb)

$D_{Ti}(m^2/s)=0.15\times10^{-4}\exp(-251200/RT)$ (in austenite), $D_{Ti}(m^2/s)=3.15\times10^{-4}\exp(-248000/RT)$ (in ferrite)
$D=f_\gamma D_\gamma+f_\alpha D_\alpha$, $\sigma_{Ti\,(C,N)}=0.8J/m^2$

Comparison of precipitated fraction of Nb (casting+reheating)

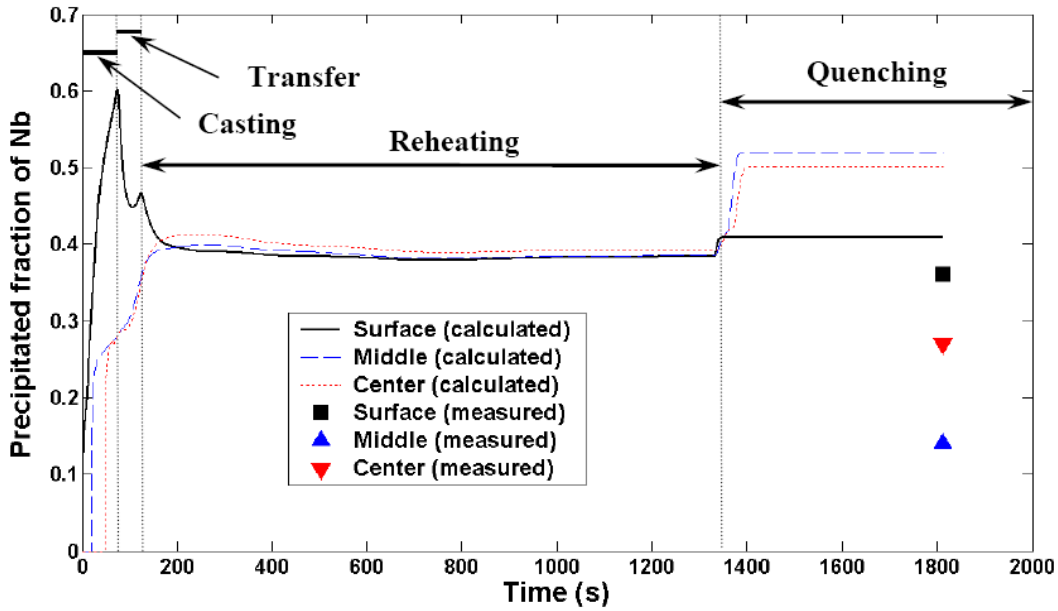

Comparison of size distributions from measurement and calculated results (casting+reheating)

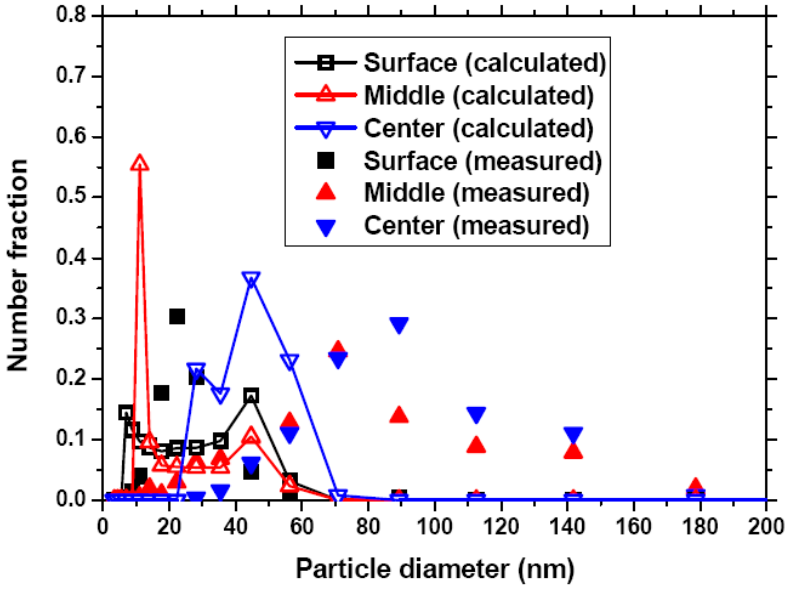

- The calculated particle diameter is around 40-50nm, which is still less than measurements for middle and center
- Better match: need precipitation on grain boundaries and segregation, more accurate temperature prediction

Molar fraction of Ti/(Ti+Nb) for different particles

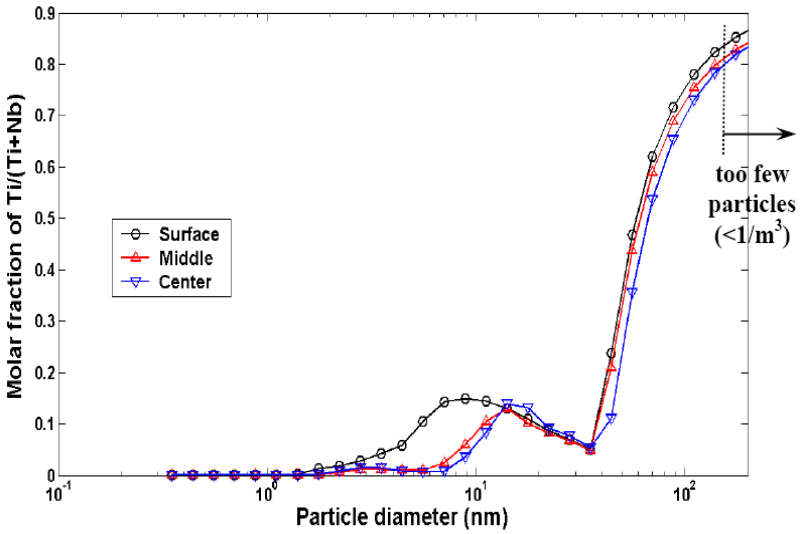

- The molar fraction Ti/(Ti+Nb) is large for large particles. It shows the Ti precipitation is the reason to form large particles
- A peak fraction around 10-20nm is likely due to secondary precipitation during quenching

EDS analysis results

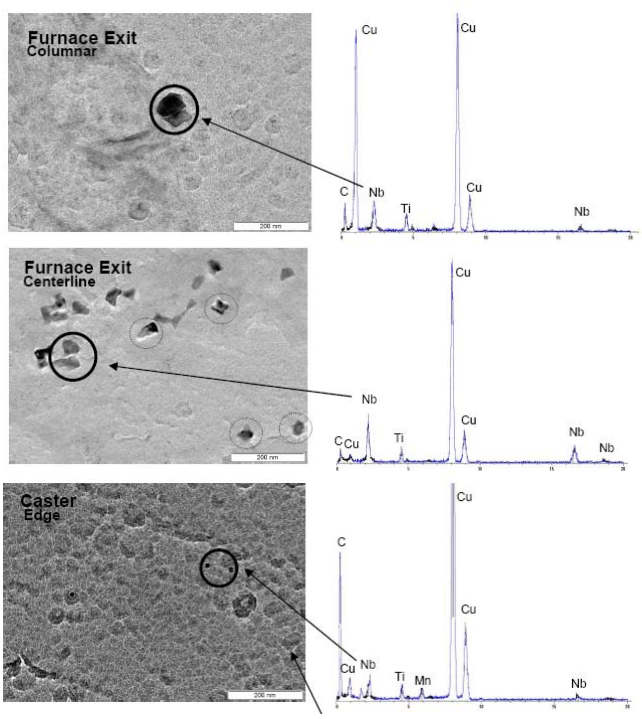

- There is always a small amount of Ti detected for all precipitate particles
- Sometimes Mn is also detected, which means large MnS particles are maybe included in measurement

Austenite grain growth prediction

Fully austenite temperature 1381.8°C, PDAS are 192μm, 470μm and 585μm separately according to cooling rates of 470°C/s, 5.66°C/s and 1.96°C/s from the slab surface to center

For a size distribution of precipitates, the limiting size is calculated by

$$\bar{D}_{\lim} = 8 / \left(3 \times \sum_i (f(r_i)/r_i) \right)$$

The summation covers the particles larger than the smallest size that exerts pinning, and the grain growth is completely inhibited when the critical size decreases to be smaller than the real grain size (pinning force>driving force)

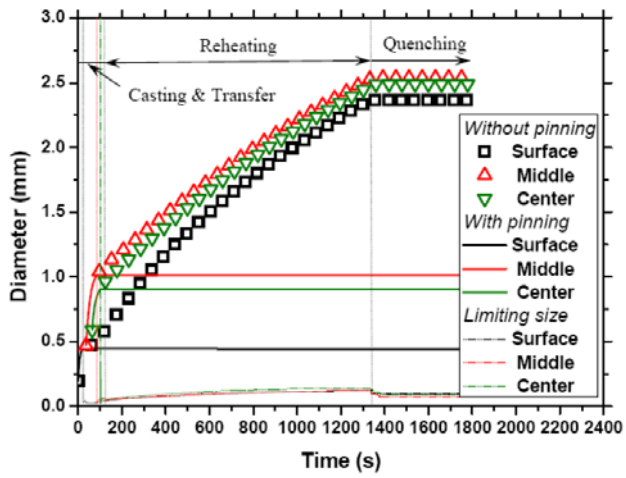

- **Without precipitate pinning, the grains are too large, and possibly cause cracks**
- **The grain growth of 3 locations are completely inhibited in reheating due to precipitate pinning**

Temperature history (casting)

- **Casting→Transfer→Quenching**
- **After the end of spray cooling, slab is air cooled for 4m, then finally water quenched to room temperature 25°C**

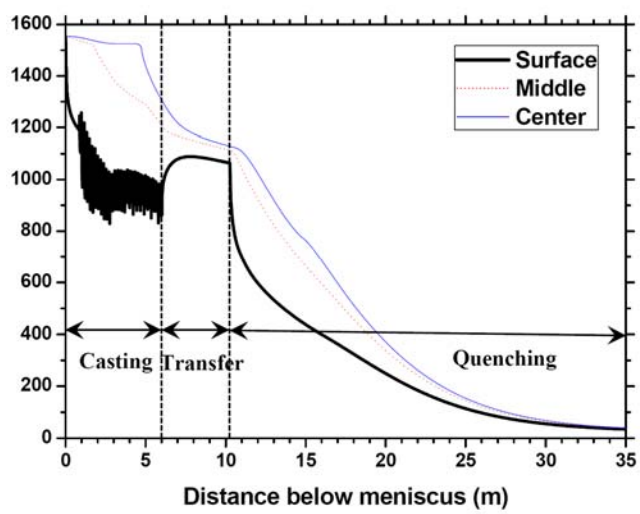

Particle size distribution (casting)

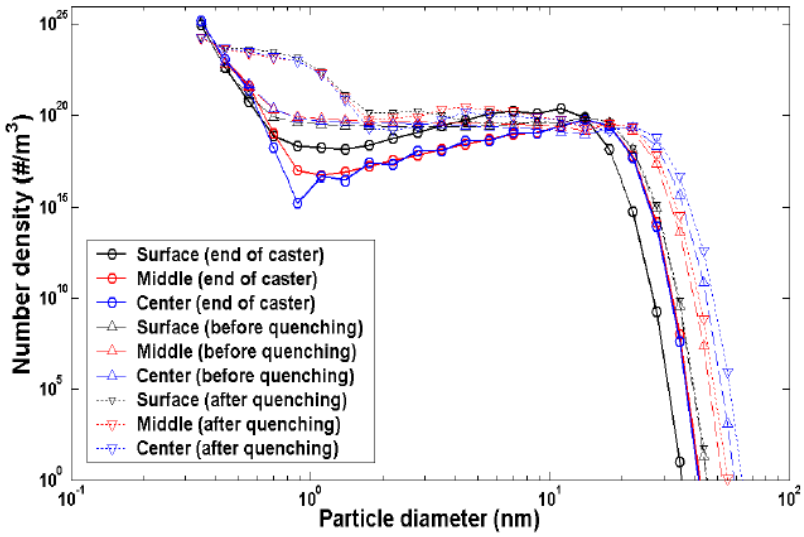

- The calculated precipitate size increase from edge to centerline, which matches the trend of measurements

Comparison of precipitated fraction of Nb (casting)

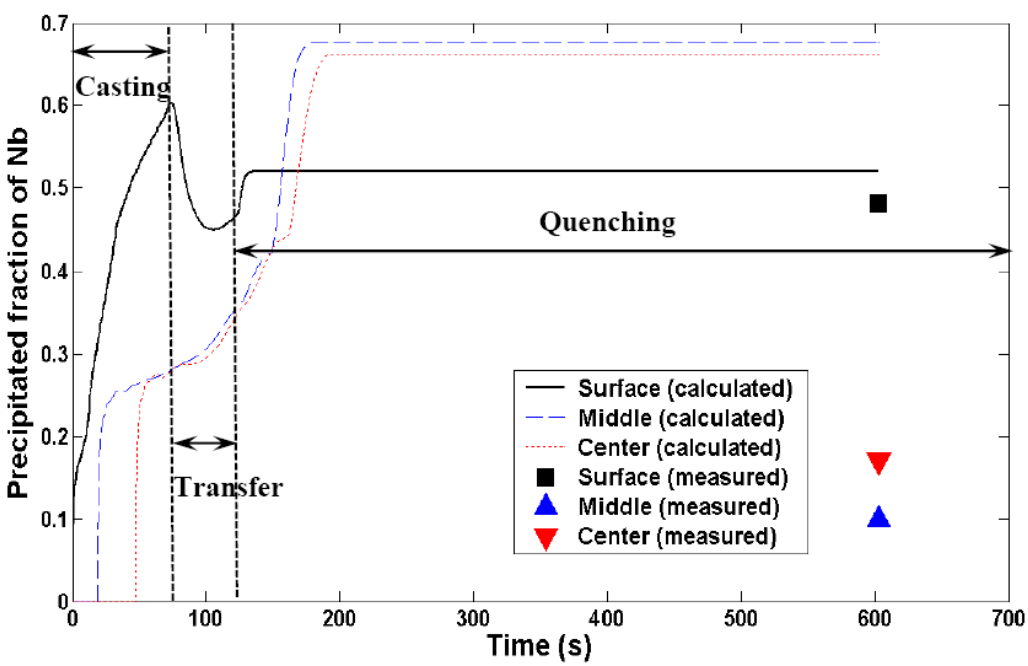

Comparison of size distributions from measurement and calculated results (casting)

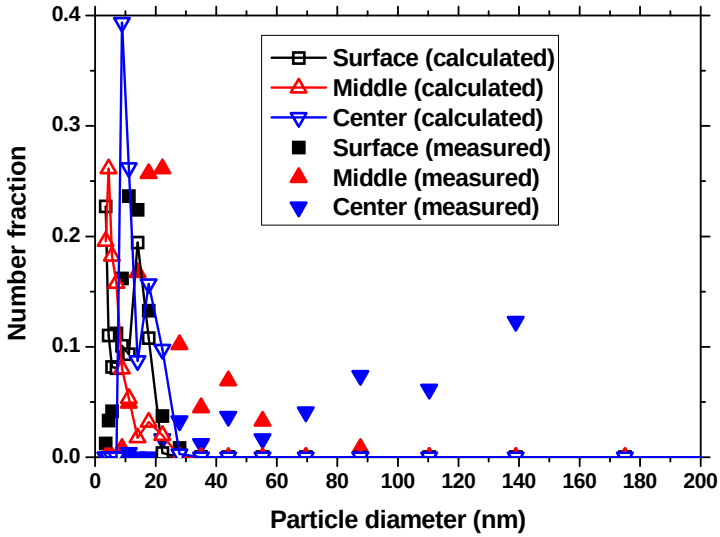

- Close match at slab surface, but still much smaller predicted size for slab interior

Conclusions

1. A fundamentally-based model of precipitate formation in practical steel processes has been developed, which includes

- Heat transfer model to predict temperature and steel phase histories
- Equilibrium precipitation model to predict equilibrium precipitate phases and amounts
- Multiphase kinetic model for predicting the evolution of the precipitate size distribution and average molar fractions of precipitate phases

2.The single Nb(C,N) model nderpredicts the measured size distributions for all edge, columnar, and centerline regions. The predicted trend of decreasing precipitate size from edge to centerline is also contrary to the measurements.

3. Multiphase (Ti,Nb)(C,N) model shows potential ability to match precipitate size measurements. A small addition of Ti is important to change precipitation behavior of Nb(C,N). Large precipitates mainly have more Ti, and small ones have more Nb.

Future work

1. Model development

- Include segregation and collision model
- Precipitation on grain boundaries (fast diffusion, curvature of grain size, segregation, different interface energy)
- Combined with stress analysis to predict cracks

2. Apply the models to locations under oscillation marks, where transverse cracks are mostly likely to occur. The higher temperature due to heat flow resistance across gap there will result in a faster grain growth rate, a lack of precipitate pinning and low ductility.

3. The models can be applied to simulate precipitation in other systems, such as Al_3Zr and Al_3Sc in aluminum alloys.

Acknowledgements

- Continuous Casting Consortium Members (ABB, ArcelorMittal, Baosteel, Tata Steel, Goodrich, Magnesita Refractories, Nucor Steel, Nippon Steel, Postech/ Posco, SSAB, ANSYS-Fluent)

- Colorado School of Mines, M.S. Dyer, J.G. Speer, D. K. Matlock